CONF-941115--5

Note: This is a preprint of a paper being submitted for publication. Contents of this paper should not be quoted nor referred to without permission of the author(s).

To be submitted to Fall 1994 Materials Research Society Meeting, Symposium F: Microcrystalline and Nanocrystalline Semiconductors, ed. by L. Brus, R. W. Collins, M. Hirose, and F. Koch.

COMPOUND SEMICONDUCTOR NANOCRYSTALS FORMED BY SEQUENTIAL ION IMPLANTATION

C. W. WHITE, J. D. BUDAI, J. G. ZHU,
S. P. WITHROW, R. A. ZUHR, and Y. CHEN
Oak Ridge National Laboratory
Oak Ridge, TN

D. M. HEMBREE, JR
The Y-12 Plant
Oak Ridge, TN

R. H. MAGRUDER
Vanderbilt University
Nashville, TN

D. O. HENDERSON
Fisk University
Nashville, TN

Prepared by the
Oak Ridge National Laboratory
Oak Ridge, Tennessee 37831
managed by
MARTIN MARIETTA ENERGY SYSTEMS, INC.
for the
U.S. DEPARTMENT OF ENERGY
under contract DE-AC05-84OR21400

November 1994

COMPOUND SEMICONDUCTOR NANOCRYSTALS FORMED BY SEQUENTIAL ION IMPLANTATION

C. W. WHITE,* J. D. BUDAI,* J. G. ZHU,* S. P. WITHROW,* R. A. ZUHR,* Y. CHEN,* D. M. HEMBREE, Jr.,** R. H. MAGRUDER,‡ AND D. O. HENDERSON‡‡

*Oak Ridge National Laboratory, P. O. Box 2008, Oak Ridge, TN 37831-6057
**The Y-12 Plant, P. O. Box 2009, Oak Ridge, TN 37831
‡Vanderbilt University, 24th Avenue S and Garland, Nashville, TN 37212
‡‡Fisk University, Physics Department, Nashville, TN 37208

ABSTRACT

Ion implantation and thermal processing have been used to synthesize compound semiconductor nanocrystals (SiGe, GaAs, and CdSe) in both SiO_2 and (0001) Al_2O_3. Equal doses of each constituent are implanted sequentially at energies chosen to give an overlap of the profiles. Subsequent annealing results in precipitation and the formation of compound nanocrystals. In SiO_2 substrates, nanocrystals are nearly spherical and randomly oriented. In Al_2O_3, nanocrystals exhibit strong orientation both in-plane and along the surface normal.

INTRODUCTION

In recent years, considerable interest has been generated in nanometer size semiconductor nanocrystals which have unique properties resulting from quantum confinement in systems of reduced linear dimensions. Much of this interest occurs because of the possibility for fabricating optoelectronic devices and optical amplifiers. The elemental semiconductor nanocrystals Si and Ge exhibit room-temperature visible-light emission at energies greater than the bandgap of the bulk semiconductor.[1-4] Intense light emission is also observed in the visible region from porous Si.[5] Compound semiconductor nanocrystals can have nearly discrete electronic states[6] and exhibit very large third-order nonlinear optical properties and fast relaxation times,[7] making them very interesting for possible applications in optical switching devices. Because of the very unusual properties associated with semiconductor nanocrystals, numerous techniques are being used to synthesize such nanocrystaline materials. These include cosputtering (to form Ge[2], Si,[8] and II–VI compound semiconductor[9,10] nanocrystals in SiO_2), plasma decomposition of SiH_4 to form Si nanocrystals,[1] organometallic reaction to form compound semiconductor nanocrystals,[11] etc.

Ion implantation is ideally suited for the fabrication of very high densities of nanocrystals in the near-surface region of a wide variety of materials and this method has been used to create Si or Ge nanocrystals in SiO_2.[12,13] We are exploring the use of ion implantation to form a wide variety of nanocrystals in several insulating materials. We have demonstrated[14,15] that implantation can be used to synthesize Si and Ge nanocrystals in both SiO_2 and Al_2O_3. In this paper, we report the synthesis of compound semiconductor nanocrystals in SiO_2 and Al_2O_3 by sequential implantation of the individual constituents of the compound, at energies chosen to give an overlap of the profiles. If the individual constituents are insoluble in the matrix, and if they have a chemical affinity for each other, then precipitation and compound formation can occur during subsequent annealing. We show results for SiGe, GaAs, and CdSe in the two substrates. This is the first report, to our knowledge, of the use of sequential implantation to form compound semiconductor nanoparticles. Previously, sequential implantation of metal ions was used to form ternary metal silicides in silicon.[16] In addition, the alloying of metal ions sequentially implanted into SiO_2 has been inferred from shifts in the wavelength of the surface plasmon resonance.[17]

EXPERIMENTAL DETAILS

The individual constituents of the desired compound semiconductor were implanted sequentially at the proper stoichiometric ratio. Substrates used were fused silica, thermally grown SiO_2 films (~8000 Å thick) on (001) Si, and (0001) Al_2O_3 crystals. Energies were chosen for each ion specie to ensure an overlap of the profiles. Doses were in the range of $3 \times 10^{16}/cm^2$ to $3 \times 10^{17}/cm^2$ for each specie. Substrate temperatures ranged from room temperature to 650°C. Following implantation, annealing was carried out in a reducing atmosphere (Ar + 4% H_2) for 1 h at temperatures in the range of 600°C to 1100°C. Sample characterization was carried out using x-ray diffraction ($CuK\alpha_1$ radiation), cross-section transmission electron microscopy (TEM), Raman spectroscopy (488 nm excitation) as well as Rutherford backscattering-ion channeling to monitor the impurity depth profile and crystallinity in the near-surface region. Optical properties of selected nanocrystal composites were determined using visible, UV, and infrared absorption as well as photoluminsescence measurements.

RESULTS AND DISCUSSION

Figure 1 shows a cross-section TEM micrograph and particle size distribution measured for SiGe nanocrystals in SiO_2. In this case, Si ions (215 keV) and Ge ions (500 keV) were implanted into SiO_2 to give an impurity profile peaked at a depth of ~3100 Å with a full width at half maximum of ~2500 Å for each constituent. Following implantation, the sample was annealed at 1000°C to induce precipitation and nanocrystal formation. X-ray diffraction showed strong diffraction lines characteristic of randomly oriented, diamond cubic SiGe, and the Raman spectrum from this sample was similar to that measured from bulk SiGe. These techniques identify the nanoparticles as a SiGe alloy, but Si and Ge are completely soluble in each other, and there is almost certainly a range of compositions in the alloy. The lack of x-ray diffraction lines and Raman lines characteristic of pure Si or pure Ge shows that there are few, if any, precipitates of the pure phase of each constituent. The TEM results show the individual SiGe nanocrystals. The size distribution is peaked at ~50 Å with a few precipitates having diameters as large as 200 Å. It should be possible to produce smaller nanocrystals and a narrower distribution by using lower doses or lower annealing temperatures as demonstrated in our work[15] on Ge nanocrystals in SiO_2. SiGe nanocrystals have also been produced in Al_2O_3 by the implantation of Si and Ge, followed by annealing. In that case, the nanocrystals are oriented preferentially with their (111) planes parallel to (0001) Al_2O_3 planes. These nanocrystals also exhibit strong in-plane alignment. Details will be published separately.

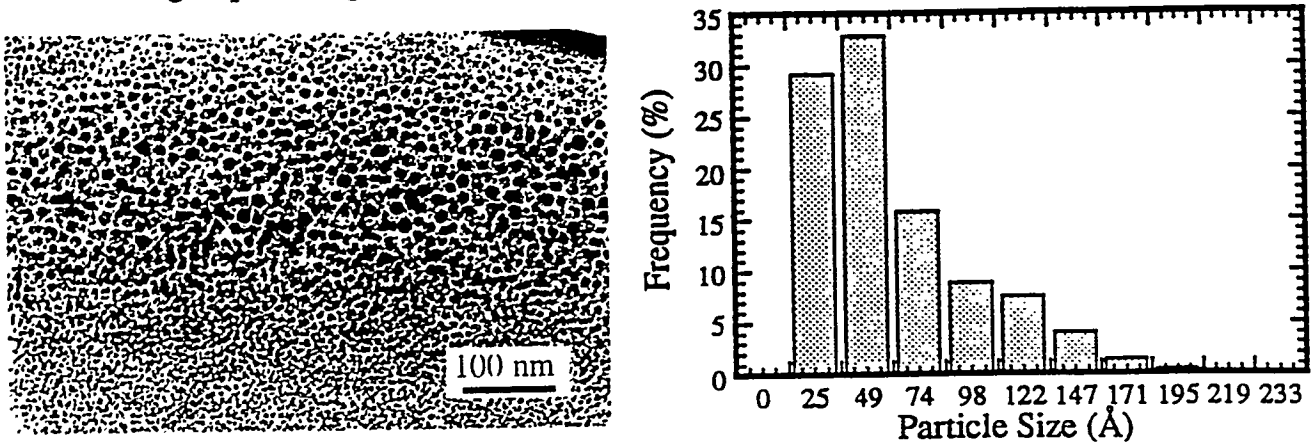

Fig. 1. (left) SiGe nanocrystals in SiO_2. Equal doses ($3 \times 10^{17}/cm^2$) of each constituent were implanted at energies chosen to give an overlap of the profile. (right) Measured size distribution for the SiGe nanocrystals.

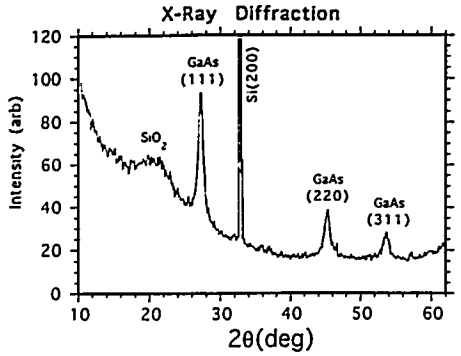

Fig. 2. X-ray diffraction characterization of GaAs nanocrystals in SiO_2. Equal doses ($1.5 \times 10^{17}/cm^2$) of Ga (at 470 keV) and As (at 500 keV) were implanted into an SiO_2/Si substrate. Annealing was carried out at 1000°C (1 h).

Nanocrystals of GaAs have also been synthesized in SiO_2 and Al_2O_3 by sequential implantation of equal doses of Ga and As, followed by thermal annealing to induce precipitation and compound formation. Figure 2 shows x-ray diffraction results for the case of GaAs nanocrystals in SiO_2. The θ-2θ scan in Fig. 2 shows the expected scattering from amorphous SiO_2 and a relatively strong multiple-scattering Si (200) peak from the underlying Si substrate. In addition, there are strong peaks which are identified as arising from diamond cubic GaAs. The intensities of these reflections are consistent with those for a randomly oriented powder. The width of these peaks provides information on the volume-weighted correlation length (size of coherently diffracting domains) which, in this case, is of order 140 Å in the direction of the surface normal. TEM results from this same sample show that the GaAs nanoparticles are nearly spherical and randomly oriented. The average size is ~100 Å diameter, with a few extending up to ~250 Å in diameter. Infrared reflectance measurements on similar samples show a well-defined peak at 280 cm^{-1} which we believe corresponds to the longitudinal optical mode of GaAs in these nanoparticles since it is close to that measured by others for bulk and epitaxial GaAs films.[19]

Figure 3 shows x-ray diffraction results for the case of GaAs nanocrystals in (0001) Al_2O_3. The θ-2θ scan (top) along the c axis of Al_2O_3 shows the expected strong diffraction from (0001) planes of Al_2O_3. In addition, there are strong diffraction peaks from (111) GaAs planes, as well as (weaker) diffraction from (110) GaAs. The intensity ratios show that the GaAs nanoparticles have a tendency to orient with their (111) planes parallel to the (0001) planes of Al_2O_3. The width of the GaAs (111) peak suggests a GaAs grain size of ~370 Å along the surface normal. The (111) oriented GaAs domains also exhibit strong in-plane alignment as shown by the φ scans through the {200} reflections. The φ scan results show that there are several possible in-plane orientations for the GaAs domains.

CdSe nanocrystals have also been synthesized in SiO_2 and Al_2O_3. Figure 4 shows a TEM image from CdSe nanocrystals in SiO_2. In this sample, the CdSe nanoparticles are nearly spherical, randomly oriented, and have an average size of ~50 Å. A few extend to diameters of 100 Å.

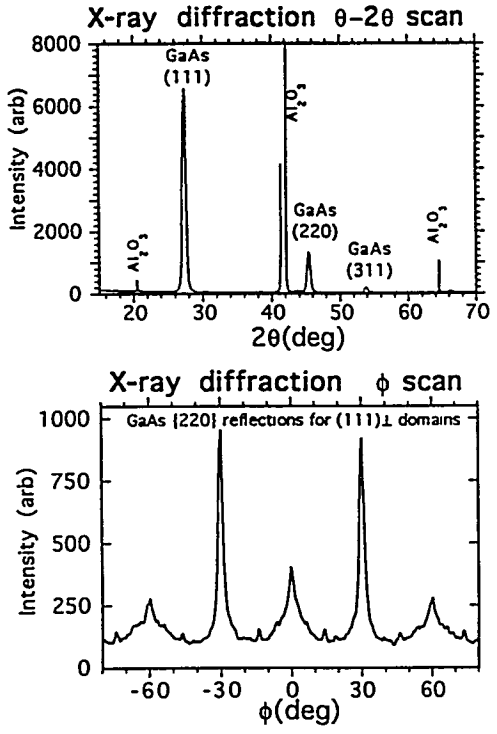

Fig. 3. X-ray diffraction from GaAs nanocrystals in (0001) Al_2O_3. Equal doses $1 \times 10^{17}/cm^2$) of Ga (at 470 keV) and As (at 500 keV) were implanted, and the sample was annealed at 1100°C/1 h.

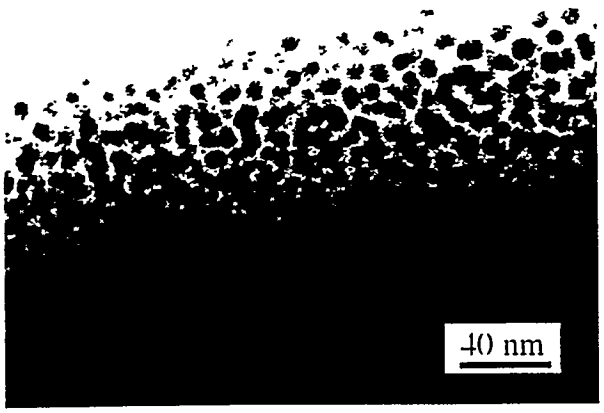

Fig. 4. CdSe nanocrystals in SiO_2. Equal doses ($1 \times 10^{17}/cm^2$) of Cd (at 450 keV) and Se (at 330 keV) were implanted and the sample was annealed at 1000°C/1 h.

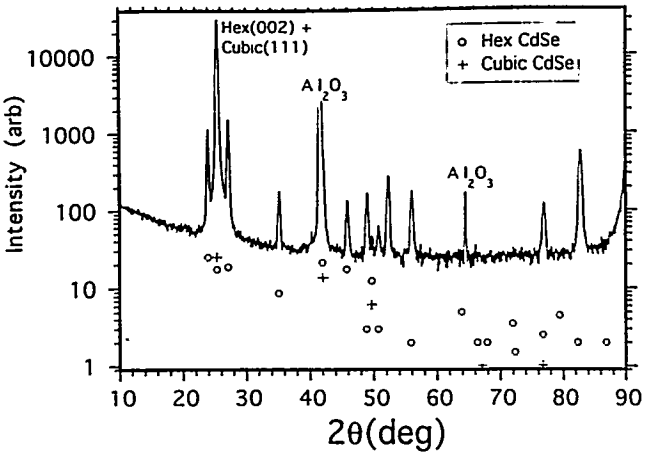

Fig. 5. X-ray diffraction from CdSe nanocrystals in (0001) Al_2O_3. Equal doses ($4.3 \times 10^{16}/cm^2$) of Cd (450 keV) and Se (330 keV) were implanted at a substrate temperature of 600°C. The sample was annealed at 1000°C/1 h.

Equilibrium CdSe exists in one of two structures, cubic and hexagonal, depending on pressure. The x-ray diffraction results from this sample reveal the presence of hexagonal CdSe, similar to results[18] reported for CdSe nanocrystals synthesized in SiO_2 by cosputtering. However, because of overlapping diffraction peaks, we cannot rule out the possibility that a small amount of cubic CdSe is also present in the implanted samples.

Figure 5 shows x-ray diffraction results demonstrating that oriented CdSe nanocrystals have been formed in Al_2O_3 by sequential implantation followed by annealing. The θ-2θ scans along the c axis show the expected scattering from Al_2O_3, along with numerous peaks which are consistent with those expected from CdSe. The expected position and relative intensities (from the powder diffraction files) of peaks arising from hexagonal and cubic CdSe are shown also in Fig. 5. From these data, the nanocrystals are identified as hexagonal, although there may be small amounts of the cubic phase present. The hexagonal CdSe (002) planes are strongly oriented parallel to the (0001) planes of Al_2O_3, and ϕ scans for these domains exhibit strong in-plane sixfold alignment. (Relative intensities of the lines in Fig. 5 will not agree with the predictions of power diffraction lines because these nanocrystals are strongy oriented.) Figure 6 shows a TEM image for this sample. This micrograph shows one isolated and several overlapping hexagonal shaped CdSe nanocrystals. Dimensions parallel to the c planes of Al_2O_3 are several hundred angstroms, and along the c axis are ~200 Å, consistent with the widths of the diffraction lines. The CdSe nanocrystals in this sample are mostly in the hexagonal phase. However, CdSe nanoparticles have been synthesized also in the cubic phase using different implantation and annealing conditions in Al_2O_3. Details will be published separately.

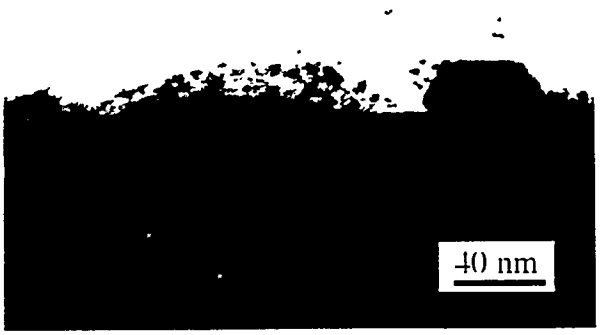

Fig. 6. CdSe nanocrystals in (0001) Al_2O_3. This is the same sample as that of Fig. 5.

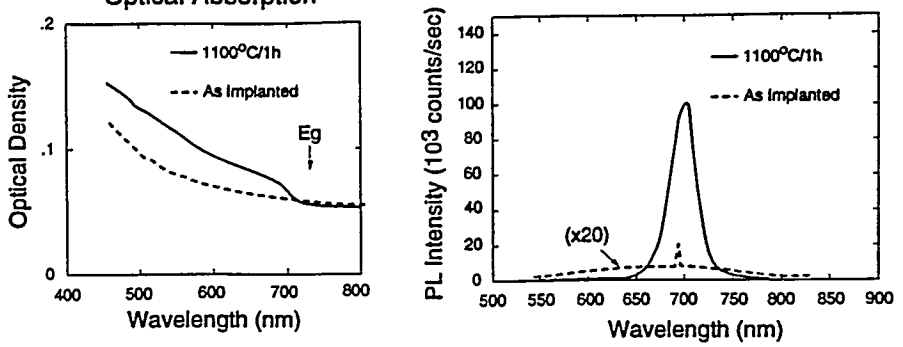

Fig. 7. Optical properties of CdSe nanocrystals in (0001) Al_2O_3. This is the same sample as that of Fig. 5.

Experiments to determine the optical properties of these compound semiconductor nanocrystal composites have just been initiated. One result is shown in Fig. 7 for the CdSe nanocrystals in Al_2O_3. The optical absorption results show a blue shift of ~0.1 eV relative to the bandgap (1.7 eV) of bulk CdSe. Such a shift is consistent with the absorption results reported in ref. 11 for the large CdSe nanoparticles (~115 Å diameter) in that study. In addition, intense band edge photoluminescence is observed as shown in Fig. 7b. Both the shift in optical absorption and the wavelength of the band edge luminescence should be strong functions of the nanocrystal size. Experiments to demonstrate this behavior are in progress.

CONCLUSIONS

Ion implantation followed by thermal processing has been used to synthesize a variety of compound semiconductor nanocrystals in both SiO_2 and Al_2O_3. Supersaturated solutions of individual constituents are created by sequential implantation at energies chosen to give an overlap of the profiles and at doses chosen to give the desired stoichiometry. If both implanted constituents are insoluble in the matrix, and if the constituents have a chemical affinity for each other, then thermal annealing gives rise to precipitation and the formation of compounds. Results are demonstrated for the case of SiGe, GaAs, and CdSe in the two matrices. In SiO_2, the nanocrystals are nearly spherical, randomly oriented, and have diameters ranging from 20–300 Å. In Al_2O_3, nanocrystals are strongly oriented with the matrix. It should be possible to synthesize a very broad range of nanocrystals in a wide variety of host materials by using the sequential implantation method.

ACKNOWLEDGMENTS

Research at ORNL was supported partly by the Division of Materials Sciences, U.S. Department of Energy, under contract DE-AC05-84OR21400 with Martin Marietta Energy Systems, Inc. and partly through the ORISE Postdoctoral Program. Research at Vanderbilt was supported by Army Research Office grant DAAH04-93-G-0123. Research at Fisk University was supported by DOE through grant DE-FG05-94ER45521.

REFERENCES

1. H. Takagi, H. Ogawa, Y. Yamazaki, A. Ishizaki, and T. Nakagiri, *Appl. Phys. Lett.* **56**, 2379 (1990).

2. Y. Maeda, N. Tsukamoto, Y. Yazawa, Y. Kanemitsu, and Y. Masumoto, *Appl. Phys. Lett.* **59**, 3168 (1991).

3. W. L. Wilson, P. F. Szajowski, and L. E. Brus, *Science* **262**, 1242 (1993).

4. L. Brus, *J. Phys. Chem.* **98**, 3575 (1994).

5. L. T. Canhan, *Appl. Phys. Lett.* **57**, 1046 (1990).

6. L. Brus, *Appl. Phys. A* **53**, 465 (1991).

7. R. K. Jain and R. C. Lind, *J. Opt. Soc. Am.* **73**, 647 (1983).

8. S. Hayashi, T. Nagareda, Y. Kanzawa, and K. Yamamoto, *Jpn. J. Appl. Phys.* **32**, 3840 (1993).

9. K. Tsunetomo, H. Nasu, H. Kitayama, A. Kawabucki, Y. Osaka, and K. Takiyama, *Jpn. J. Appl. Phys.* **28**, 1928 (1989).

10. B. G. Potter and J. H. Simmons, *J. Appl. Phys.* **68**, 1218 (1990).

11. C. B. Murray, D. J. Norris, and M. G. Bawendi, *J. Am. Chem. Soc.* **115**, 8706 (1993).

12. H. Atwater et. al., *Mat. Res. Soc. Sym. Proc.* **316**, 409 (1994).

13. T. Shimizu-Iwayama, K. Fujita, S. Nakao, K. Saitoh, T. Fujita, and N. Itoh, *J. Appl. Phys.* **75**, 7779 (1994).

14. C. W. White et al., *Mat. Res. Soc. Sym. Proc.* **316**, 487 (1994).

15. J. G. Zhu et al., these proceedings; J D. Budai et al., these proceedings.

16. Z. Tan, F. Namavar, S. M. Heald, and J. Budnick, *Appl. Phys. Lett.* **63**, 791 (1993).

17. R. H. Magruder, J. E. Wittig, and R. A. Zuhr, *J. Non Cryst. Solids* **163**, 162 (1993); R. A. Zuhr, R. H. Magruder, T. A. Anderson, and J. E. Wittig, *Mat. Res. Soc. Sym. Proc.* **316**, 457 (1994).

18. K. Tsunetomo, A. Kawabuchi, H. Kitayama, Y. Osaka, and H. Nasu, *Jpn. J. Appl. Phys.* **29**, 2481 (1990).

19. R. T. Holm, J. W. Gibson, and E. D. Palik, *J. Appl. Phys.* **48**, 212 (1976).